LOW LOSS TUNABLE OPTICAL FILTER USING SILICON PHOTONIC BAND GAP MIRRORS

Ariel Lipson and Eric M. Yeatman
Department of Electrical & Electronic Engineering, Imperial College London, U.K.
(Tel: +44-20-7594-6204; E-mail: e.yeatman@imperial.ac.uk)

Abstract: A fiber-pigtailed tunable optical filter is described, based on silicon-air photonic bandgap mirrors. The high reflectance achievable in these mirrors allows a short Fabry-Perot cavity to be employed, such that lensed fibers provide sufficient collimation without additional focusing elements. Mirror surface orientation and quality are shown to be crucial to performance, and a two-stage etch process is used to satisfy this requirement. MEMS elecrostatic actuation of one mirror is used for tuning, and the final device achieves fiber-to-fiber insertion loss of 11 dB, passband width 3 nm, and tuning range ≈ 10 nm.

Keywords: tuneable filter, anisotropic etching, MEMS

I. INTRODUCTION

Periodic structures such as gratings and thin-film multi-layers are the basis of many optical filters, particularly when a high degree of spectral selection is needed. When mechanical actuation is added, such filters become tunable, and MEMS is an attractive approach to providing this tunability in an integrated device. Previously, MEMS tunable filters have been demonstrated based on vertical actuation, or rotation of multi-layers deposited on the wafer surface [1]. However, this requires an optical axis perpendicular to the surface, which makes accurate integration with optical fibers difficult. Placing the optical axis in the wafer plane allows the provision of grooves for fiber insertion and alignment, and also means that periodic structures can be produced by etching an appropriate pattern of holes or slits into the dielectric. Because of their high refractive index contrast, such dielectric-air structures require fewer periods, and are frequently referred to as photonic band-gap (PBG) devices.

We have designed, fabricated and tested a fiber-pigtailed tunable filter suitable for optical communications, based on a Fabry-Perot cavity with silicon-air PBG mirrors. A free space beam propagates through the filter structure between lensed fibers, and one mirror is translated electro-statically to provide tuning. Fig. 1 shows a schematic of the operating principle, and Fig. 2 and Fig. 3 show the completed device before fiber attachment.

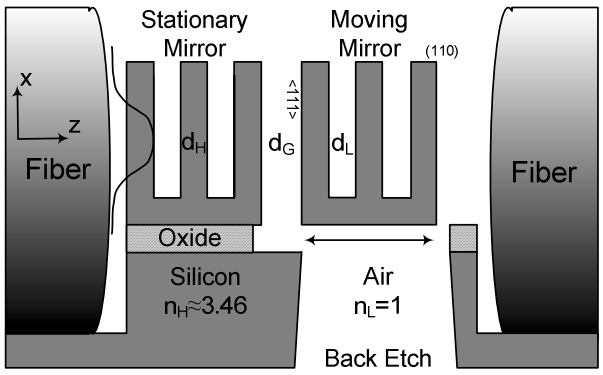

Fig. 1: Schematic of PBG filter (elevation view).

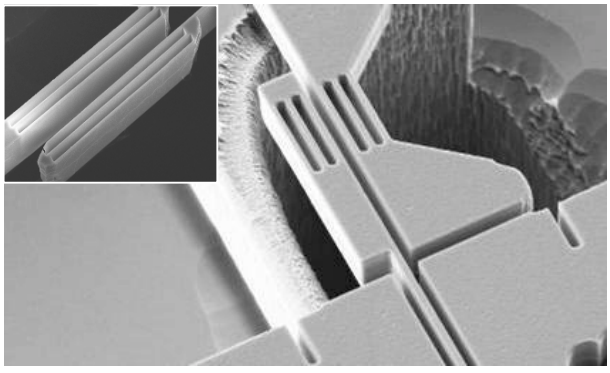

Fig. 2: Detail of fabricated PBG mirror pair after release, before fiber attachment. Inset shows a close-up of mirrors after KOH etching.

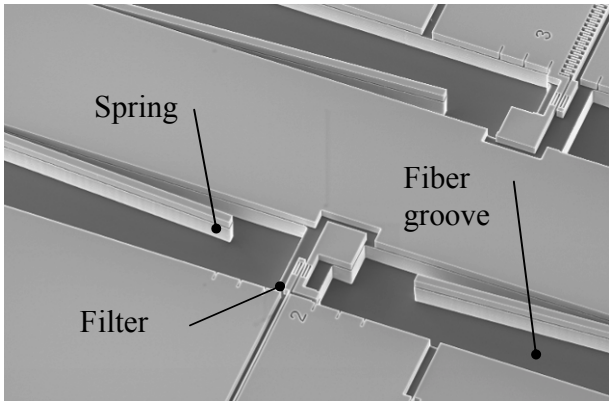

Fig. 3: Overview of the device including the filter, actuator, fiber grooves and alignment springs.

Although Si can be etched with high precision, isotropic dry etching cannot give sufficient mirror quality. Simulation of filter pass-band shape vs. mirror verticality shows that an angle below 0.01° is essential, and experimental results show that we have achieved this. The key fabrication difficulty is achieving sufficient mirror quality, in terms of the verticality, flatness and smoothness of the reflecting surfaces. This difficulty explains the high loss values seen in PBG filters based on AlGaAs waveguides [2].

II. FABRICATION AND MEASUREMENTS

Mirror fabrication was done by a two-step etch process which we have previously demonstrated for static filters [3]. First, deep reactive ion etching (DRIE) is used to define all the structures of the device. The critical mirror surfaces are aligned to the (111) planes (vertical in (110) wafers), and are then polished to these planes by a brief anisotropic KOH etch. Fig. 4 is a close-up of the cantilever anchor verifying the anisotropic etching by the presence of exposed (111) planes. Each mirror consists of 3 Si layers and 2 air slits. Release of the movable parts is done by back-etching, and a key part of the process development was to avoid damaging the mirror parts in later process steps [4]. The mirror depth is defined by the device layer of bonded silicon on insulator (BSOI) wafers, with the deeper fiber alignment grooves etched further, into the handle layer. Apart from polishing, the KOH anisotropic etch is further used to deepen the PBG mirrors down to the oxide layer, avoiding the typical notching effect of DRIE. This process promises a perfect mirror structure.

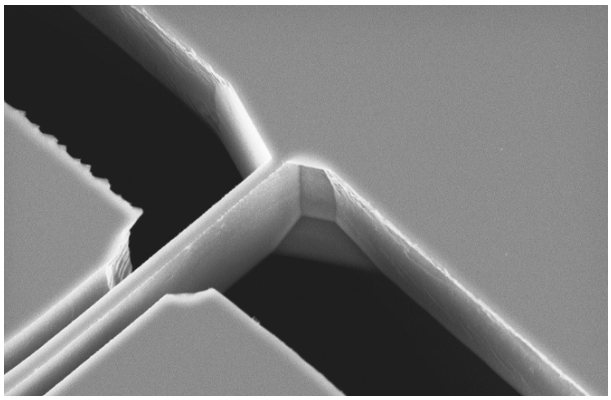

Fig. 4: Detail of the cantilever anchor after KOH etching, showing the exposed (111) planes.

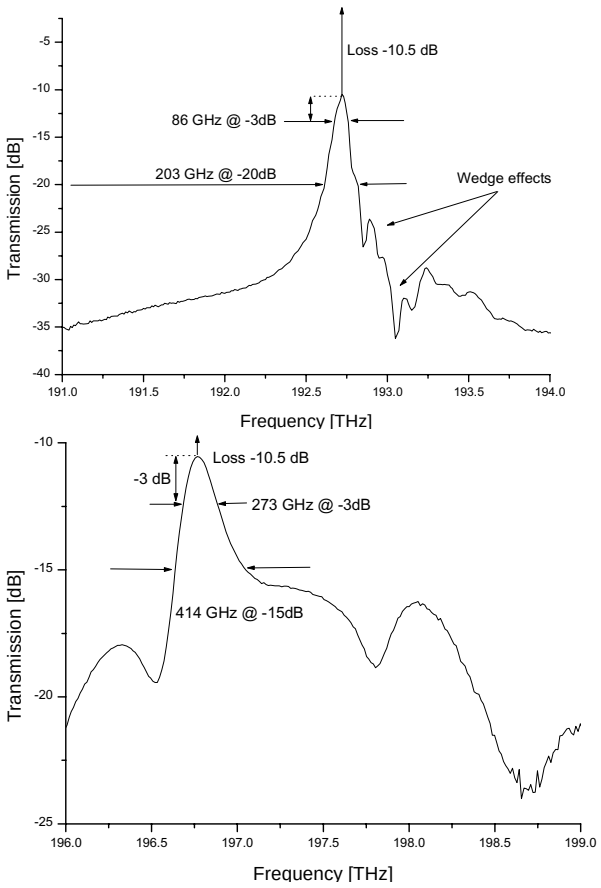

Fig. 5: Two fabricated non-released filters show quite different performance, possibly due to variations in etching angle and insufficient control of the silicon layer widths.

Fig. 5 shows the spectral response of two non-released filters. The device in the upper plot has excellent characteristics, with insertion loss of -10.5 dB, a narrow pass band of 66 GHz (0.5 nm), and a 200 GHZ channel isolation of -20dB. A 700 GHz shift in the transmission peak, compared to the design value, was observed, equivalent to a systematic 26 nm over-etching of the silicon layer widths.

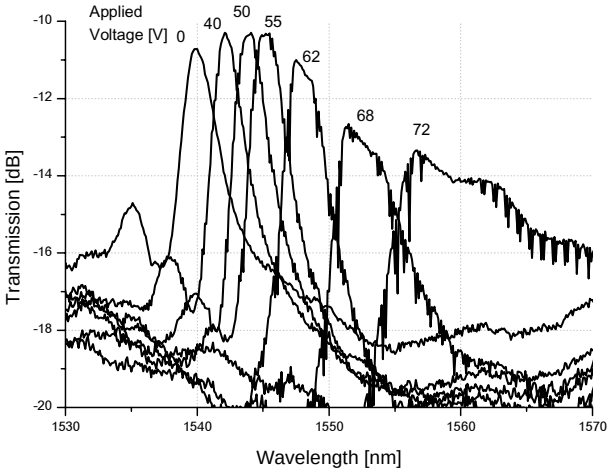

Fig. 6: Measured optical transmission, fiber-to-fiber, vs. actuation voltage, for a device with actuator cantilever length 100 μm.

Fig. 6 shows the measured optical response for two released, tunable devices. The pass band width is ≈ 6 nm, significantly more than in the static case (< 1 nm). There is some degradation with tuning because of the slight rotation of the moving mirror; this will be corrected in the next iteration using a doubly suspended actuator (see Fig. 9). The tuning range before major performance degradation is over 10 nm, and the insertion loss ≈ 11 dB. Actuation voltage is up to 70V; this can be reduced by increasing the cantilever length of the actuator (see below).

The displacement vs. voltage responses of actuator cantilevers of length 300 μm are presented in Fig. 7, for the two cases of parallel plate actuation, as used in the devices described above, and comb-drive. Since the displacement is in the range of tens of nm, image processing was used to extract the position data. Both types show an initial voltage offset before any response; this we believe is an artefact of the probe contacts. Apart from this, the comb drive gives a linear response, as expected, while the plate capacitor shows non-linear deflection and eventual snap down. For an optical network filter, the position of the cantilever must be stabilized, and therefore a linear characteristic is desired. In the process used for the current filters it is not possible to have comb-drives along with wet-etching of the mirrors, but this is to be corrected in future work, as explained in the next section.

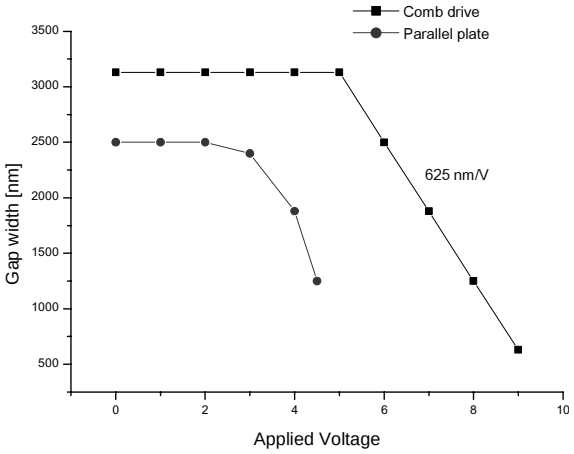

Fig. 7: Comb drive and parallel plate displacement vs. voltage measurements.

III. DESIGN CONSIDERATIONS

For optical communication networks the filter must satisfy conditions such as low loss, narrow channel width and wide stop band. Desired combinations of these parameters can be obtained by correct choice of PBG layer thicknesses. The alternating silicon and air layers are each odd multiples of quarter wavelengths in width. By assigning the notation m_i to describe the ¼λ multiplication factor for layer i, one can write the layer thicknesses for the high and low index layers d_H and d_L as:

$$d_H = \frac{1}{4} \cdot m_{si} \cdot \frac{\lambda_c}{n_{si}} \quad d_L = \frac{1}{4} \cdot m_{air} \cdot \frac{\lambda_c}{n_{air}} \quad m = 1,3,5... \qquad (1)$$

Simulations were carried out using different factors for the silicon and the air layers, m_{si} and m_{air} respectively. The cavity length is considered as two air layers. The spectrum clearly changes with the thickness alteration, yielding adjustment to the stop band width, channel width @ -20 dB, and losses.

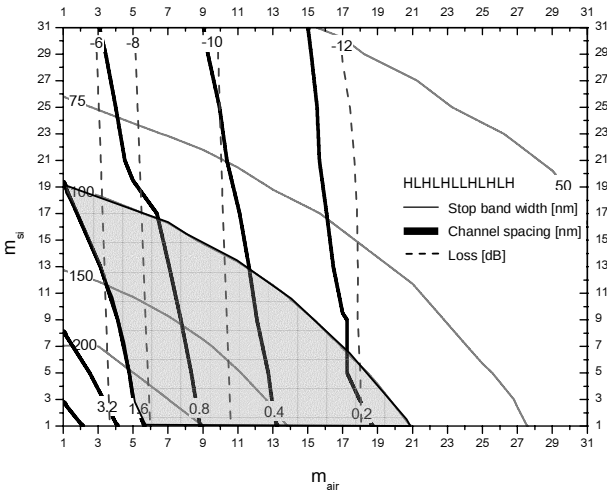

Fig. 8: Simulation of impact of layer thickness on filter characteristics. Solid thin and thick lines show stop band and channel widths, and dashed lines show the anticipated loss. The shaded area indicates the parameter zone having stop band > 100 nm and channel spacing < 1.6 nm (200 GHz).

Fig. 8 summarizes these simulations for a filter with a 9 μm wide optical beam. One can see that for at least 100 nm stop band and a channel width smaller than 1.6 nm (parameters suitable for DWDM), possible m factors are in the area under the 100 curve and to the right of the 1.6 nm line (shaded area). For fabrication reasons we chose the thickest possible silicon layers, although thinner layers should yield some loss improvement as indicated. Note that in the simulation the loss results from the finite beam width, and consequent beam spreading. Plots of this type can be used as design guides for given values of beam width, high and low refractive indices, and performance requirements, giving allowable m values in each case.

IV. CONCLUSIONS & FUTURE WORK

Improvements to the fabrication process are proposed for future work, to overcome identified deficiencies. The improvements include: (a) better width control over PBG layers using a thin nitride mask; (b) using BSOI handle layer thickness to set the fiber groove height (75 μm) rather than the less critical mirror height; (c) comb-drive actuation, for improved stability, realized by wet etching the PBG layers first and then patterning the actuator; (d) a doubly supported actuator beam to prevent angle change with tuning. Fig. 9 shows a CAD model of a filter implementing the proposed process improvements.

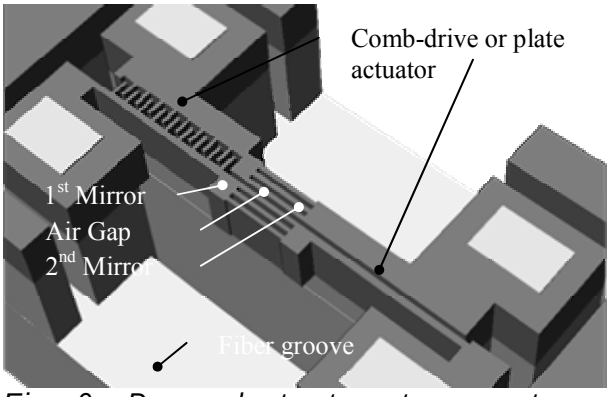

Fig. 9: Proposed structure to prevent angle dependant tuning.

In summary, we report the first fiber-connected MEMS-tunable PBG filter, based on silicon micromachining, for applications in optical communication.

REFERENCES

[1] R. H. Trimm, E. J. Tuck, G. Tuck, M. C. Buncick, M. Kranz, P. Reiner, M. G. Temmen, and P. R. Ashley, "Dynamic MEMS-based photonic bandgap filter," Sensors Journal, IEEE, vol. 5, pp. 1451-1461, 2005.

[2] D. J. Ripin, K.-Y. Lim, G. S. Petrich, P. R. Villeneuve, S. Fan, E. R. Thoen, J. D. Joannopoulos, E. P. Ippen, and L. A. Kolodziejski, "One-dimensional photonic bandgap microcavities for strong optical confinement in GaAs and GaAs/Al_xO_y semiconductor waveguides," J. Lightwave Technology, vol. 17, pp. 2152-2160, 1999.

[3] A. Lipson and E. M. Yeatman, "Low-loss one-dimensional photonic bandgap filter in (110) silicon," Optics letters, vol. 31, pp. 395-7, 2006.

[4] A. Lipson and E. M. Yeatman, "A 1-D Photonic Band Gap Tunable Optical Filter in (110) Silicon," IEEE/ASME Journal of Microelectromechanical Systems, 2007, in press.